Identification of Protein Tyrosine Phosphatases Associating with the PDGF Receptor†

Boyka Markova,‡ Peter Herrlich,§ Lars Rönnstrand,|| and Frank-D. Böhmer*,‡

Research Unit Molecular Cell Biology, Medical Faculty, Friedrich Schiller University, Drackendorfer Strasse 1, D-07747 Jena, Germany, Institute of Toxicology and Genetics, Forschungszentrum Karlsruhe, Karlsruhe, Germany, and Uppsala Branch, Ludwig Institute for Cancer Research, Uppsala, Sweden

Received August 1, 2002; Revised Manuscript Received January 9, 2003

ABSTRACT: Protein tyrosine phosphatase (PTP) in-gel assays were used to explore association of PTPs with the platelet-derived growth factor β-receptor (PDGFβR). Five PTP activity bands of ~120, ~70, ~60, ~53, and ~45 kDa could be detected in PDGFβR immunoprecipitates and were identified by immunodepletion experiments as PTP-PEST, SHP-2, an active fragment of SHP-2, PTP-1B, and T-cell PTP, respectively. The PTP pattern that was obtained was similar in PDGFβR immunoprecipitates from HEK 293 cells overexpressing the human PDGFβR and from murine fibroblasts. Association of PTP-1B with the PDGFβR was stabilized by pretreatment of the cells with hydrogen peroxide. The epidermal growth factor receptor (EGFR) immunoprecipitated from fibroblasts, and c-Kit isolated from CHRF myeloid cells, were associated with partially overlapping but quantitatively different patterns of PTPs. PTP-PEST was the predominant PTP in EGFR immunoprecipitates, and SHP-1 appeared in c-Kit immunoprecipitates. We propose that the differential association of PTPs with different RTKs is related to their respective contributions to regulation of RTK signaling.

Receptor tyrosine kinase (RTK)[1] signaling is tightly regulated. Several cellular mechanisms which prevent signaling in the absence of ligand or control attenuation or termination of signaling after ligand-dependent RTK activation have been identified (*1*). These involve Ser/Thr phosphorylation of RTKs, ubiquitin-mediated degradation of RTK, and dephosphorylation of RTK by PTPs. For most RTKs, the relative contributions of these mechanisms to regulation of signaling are not clear. However, there is genetic evidence showing that PTPs are biologically relevant negative regulators for signaling of some RTKs (*2*). As a striking example, the insulin receptor signaling in insulin-responsive tissues was strongly upregulated upon disruption of the PTP-1B gene (*3*, *4*). For the PDGF receptor, receptor dephosphorylation dominated over receptor internalization and ubiquitin-mediated receptor degradation, suggesting a major role of PTPs in the negative regulation of PDGF signaling (*5*). While analysis of cellular and animal models with genetically or functionally inactivated PTP species will provide further insight into the role of individual PTPs for certain RTK systems, there is no systematic approach for identifying those PTPs out of at least 37 known entities (*6*) which are relevant for a given RTK. PTPs, which directly dephosphorylate a RTK, should—at least transiently—bind to their substrate in the course of the dephosphorylation reaction. In addition, they might bind to a target RTK through additional binding domains, exemplified by SH2 domains which for instance direct the PTP SHP-1 to a range of targets, including RTKs c-Kit and Ros (*2*). Therefore, the specific association of a PTP with a tyrosine-phosphorylated protein can serve as an indicator of a potential enzyme−substrate interaction or an otherwise physiologically relevant interaction. Here we employed the highly sensitive PTP in-gel assay (*7*) to analyze PTPs bound to the PDGFβR, and we identified PTP-1B, TC-PTP, PTP-PEST, and SHP-2 as PTPs specifically complexing with the PDGFβR. Other RTKs, analyzed for comparison, show a partially overlapping but clearly different pattern of PTP association. Our assays predict a certain redundancy of PTP−RTK interaction, which will be discussed in light of recent findings on the role of the identified PTP species for PDGFR signaling.

EXPERIMENTAL PROCEDURES

DNA Constructs and Cell Lines. Construction of an expression plasmid for the C-terminally HA-tagged human PDGFβR was described previously (*8*). The corresponding kinase-dead K634A mutant was obtained by replacing nucleotides 1975−2799, which are flanked by unique *Sac*II and *Bst*EI restriction sites, using the corresponding DNA fragment from PDGFβR K634A (*9*) in pSV7. A HEK 293 cell line stably expressing the HA-tagged human PDGFβR was obtained by transfecting the cells with PDGFβR-encoding cDNA in the vector pNRTIS33 (*10*). HEK 293 cells were cultured in a 1:1 DMEM/F12 mixture, supplemented with 10% FCS. CHRF cells (myeloid leukemia cells; kindly provided by M. Lieberman, Cincinnati, OH) were grown in

† This work was supported by grants from Deutsche Forschungsgemeinschaft to F.-D.B. (BO 1043/4) and to P.H. (He 551/9-1 and He 551/11-1) and by the Deutsche Akademische Austauschdienst (DAAD).

* To whom correspondence should be addressed. Fax: +49-3641-304462. E-mail: i5frbo@rz.uni-jena.de.

‡ Friedrich Schiller University.

§ Forschungszentrum Karlsruhe.

|| Ludwig Institute for Cancer Research.

[1] Abbreviations: RTK, receptor tyrosine kinase; PTP, protein tyrosine phosphatase; PDGFR, platelet-derived growth factor receptor; EGFR, epidermal growth factor receptor; TC-PTP, T-cell PTP; FCS, fetal calf serum; SCF, stem cell factor; HEK 293, human embryonic kidney 293; PMSF, phenylmethanesulfonyl fluoride; pI, isoelectric point; Ip, immunoprecipitate.

10.1021/bi0265574 CCC: $25.00
Published on Web 02/14/2003

DMEM, supplemented with 10% heat-inactivated FCS, and K562 cells were grown in RPMI medium and 10% heat-inactivated FCS. Mouse embryonic fibroblasts derived from PTP-1B knockout mice, immortalized with SV 40 large T antigen and reconstituted with wild-type human PTP-1B or mock-transduced with pWZL vector control (*11*), were kindly provided by B. Neel and F. Haj (Boston, MA). These cells were cultivated in DMEM and 10% FCS.

Reagents. Mouse monoclonal anti-PTP-1B antibodies (clone FG6-1G) were purchased from Calbiochem-Novabiochem (Bad Soden, Germany). Mouse monoclonal anti-TC-PTP antibodies (clone CF4-1D) were kindly provided by N. Tonks (Cold Spring Harbor, NY). Mouse monoclonal anti-SHP-1 antibodies were obtained from Transduction Laboratories (Lexington, KY); rabbit polyclonal anti-PDGFβ receptor (958), rabbit polyclonal anti-EGF receptor (1005), rabbit polyclonal anti-c-Kit (C-19), and mouse monoclonal anti-SHP-2 (B1) antibodies were purchased from Santa Cruz Biotechnology Inc. (Santa Cruz, CA). The rabbit polyclonal anti-mouse PTP-PEST antibody (1075) was a kind gift from M. Tremblay (Montreal, PQ). Mouse monoclonal anti-HA antibodies were from Roche Diagnostics (Mannheim, Germany). Mouse monoclonal anti-phosphotyrosine antibodies (4G10) were from Upstate Biotechnology (Lake Placid, NY). IgG2a and 2b control antibodies were obtained from Sigma.

Poly(glutamic acid$_4$-tyrosine$_1$) random copolymer was purchased from Sigma. Immobiline Dry Strips for isoelectric focusing (type 3-10 L, 11 cm) were obtained from Amersham Pharmacia Biotech (Freiburg, Germany). Human recombinant PDGF-BB, EGF, and SCF were from PeproTech Inc. (Rocky Hill, NJ). Genistein was from Calbiochem-Novabiochem.

Transient Transfections. HEK 293 cells were transfected with HA-tagged human PDGFβR wild-type or K634A mutant expression constructs or mock-transfected according to the protocol of Chen and Okayama (*12*). Briefly, 10 cm dishes were transfected with 20 μg of DNA. The next day the medium was changed to a fresh DMEM/F12 mixture, supplemented with 0.5% FCS, and the cells were left for an additional 24 h before stimulation and harvesting.

Cell Stimulation and Immunoprecipitations. Cells were starved for 24 h or overnight in medium containing 0.5% FCS, and were then stimulated for 10 min at room temperature with PDGF-BB (50 ng/mL), EGF (100 ng/mL), or SCF (40 ng/mL) or left untreated. Treatment with H_2O_2 (see the figure legends) was carried out at 5 mM for 30 min at 37 °C, before addition of growth factors. Treatment with genistein was carried out for 15 min at 100 μM (final concentration) before addition of other agents. For harvesting, cells were washed with ice-cold PBS and lysed in buffer containing 50 mM HEPES (pH 7.4), 150 mM NaCl, 0.5% Nonidet P40, 1 mM EDTA, 2 mM EGTA, 20 μg/mL leupeptin, 1 μg/mL pepstatin, 200 KIE/mL aprotinin, and 1 mM PMSF. In some cases, as indicated in the figure labeling, the lysis buffer contained additionally 1 mM sodium orthovanadate. Immunoprecipitations were performed with appropriate antibodies for 4 h at 4 °C. The immunoprecipitates were washed four times in 50 mM HEPES (pH 7.4), 150 mM NaCl, 0.05% Nonidet P40, 1 mM EDTA, and 1 mM PMSF.

For some experiments, anti-PTP-1B antibodies were covalently coupled to Protein A−Sepharose beads by cross-linking with dimethylpimelimidate (*13*). To confirm the specificity of anti-SHP-2- and anti-PTP-1B antibodies, immunoprecipitates were subjected to SDS−PAGE and the identity of the candidate PTP bands was confirmed by MALDI-TOF analysis of tryptic peptides.

In-Gel PTP Assay. Detection of PTP activity in cell lysates or immunoprecipitates was performed with an in-gel PTP assay as described by Burridge and Nelson (*7*) with the following modifications. For generating the radioactive substrate, poly(Glu$_4$Tyr$_1$)$_n$ was [^{32}P]tyrosine phosphorylated using recombinant human p60^{c-src}, expressed as a GST fusion protein in *Escherichia coli*. The labeled substrate was added to the polymerization mix of a 10% standard SDS−polyacrylamide gel (30:0.8 acrylamide:bisacrylamide ratio). Instead of Tween 40, Tween 20 was used throughout. The last renaturation step was done in buffer containing 50 mM Tris-HCl (pH 7.4), 0.3% β-mercaptoethanol, 1 mM EDTA, and 0.04% Tween 20 overnight.

Two-Dimensional in-Gel PTP Assay. Components of the two-dimensional sample buffer were added as solids to 150 μL of cell lysate to give final concentrations of 7 M urea, 2 M thiourea, 4% Chaps, 1% Triton X-100, 0.8% Pharmalyte 3-10, 65 mM DTT, 20 mM Tris, and 5 mM Pefabloc in a volume of 250 μL. Ready-to-use Immobiline DryStrips were reswollen overnight in the samples prepared in the manner described above. The IEF was carried out up to a total of 50 kVh. Prior to SDS gel electrophoresis, the gel strips were incubated for 20 min in equilibration buffer [50 mM Tris-HCl (pH 6.8), 30% glycerol, 1% SDS, 6 M urea, and 54 mM DTT]. SDS−PAGE was performed in a 10% polyacrylamide gel, containing radioactively labeled poly(Glu$_4$Tyr$_1$)$_n$, and detection of PTP activity was done as described above.

Kinase Reactions with PTP-1B Immunoprecipitates. For these experiments, HEK 293 cells stably transfected with an expression construct for the HA-tagged human PDGFβR were used. Cells were starved with 0.5% FCS and treated as described in the corresponding figure legend. PTP-1B was immunoprecipitated, and immunoprecipitates corresponding to cells from two 75 cm^2 culture flasks were washed twice with kinase buffer [50 mM HEPES (pH 7.4), 5 mM $MnCl_2$, and 1 mM sodium orthovanadate] and subjected to a kinase reaction with 1 μCi of [γ-^{32}P]ATP at 30 °C for 20 min. The reactions were terminated with SDS−PAGE sample buffer and the mixtures analyzed by SDS−PAGE and autoradiography using a Fuji FLA 5000 imager.

MALDI-TOF MS Analysis. Immunoprecipitates generated with covalently coupled PTP-1B antibodies or SHP-2 antibodies were analyzed with an in-gel PTP assay. Coomassie-stained protein bands matching the activity bands were cut and subjected to in-gel tryptic digestion and peptide extraction as described previously (*14*). The peptide mixtures were analyzed by MALDI-TOF MS on a Bruker Biflex III instrument (Bruker Daltonics, Bremen, Germany). Samples were prepared as "dried droplets" using α-cyano-4-hydroxycinnamic acid as a matrix. The peptide mass fingerprinting analysis was done using ProFound version 4.10.5.

RESULTS

PTPs Associating with the PDGFβR. To visualize PTPs, which associate with the PDGFβR, HEK 293 cells were transiently transfected with an HA-tagged PDGFβR expres-

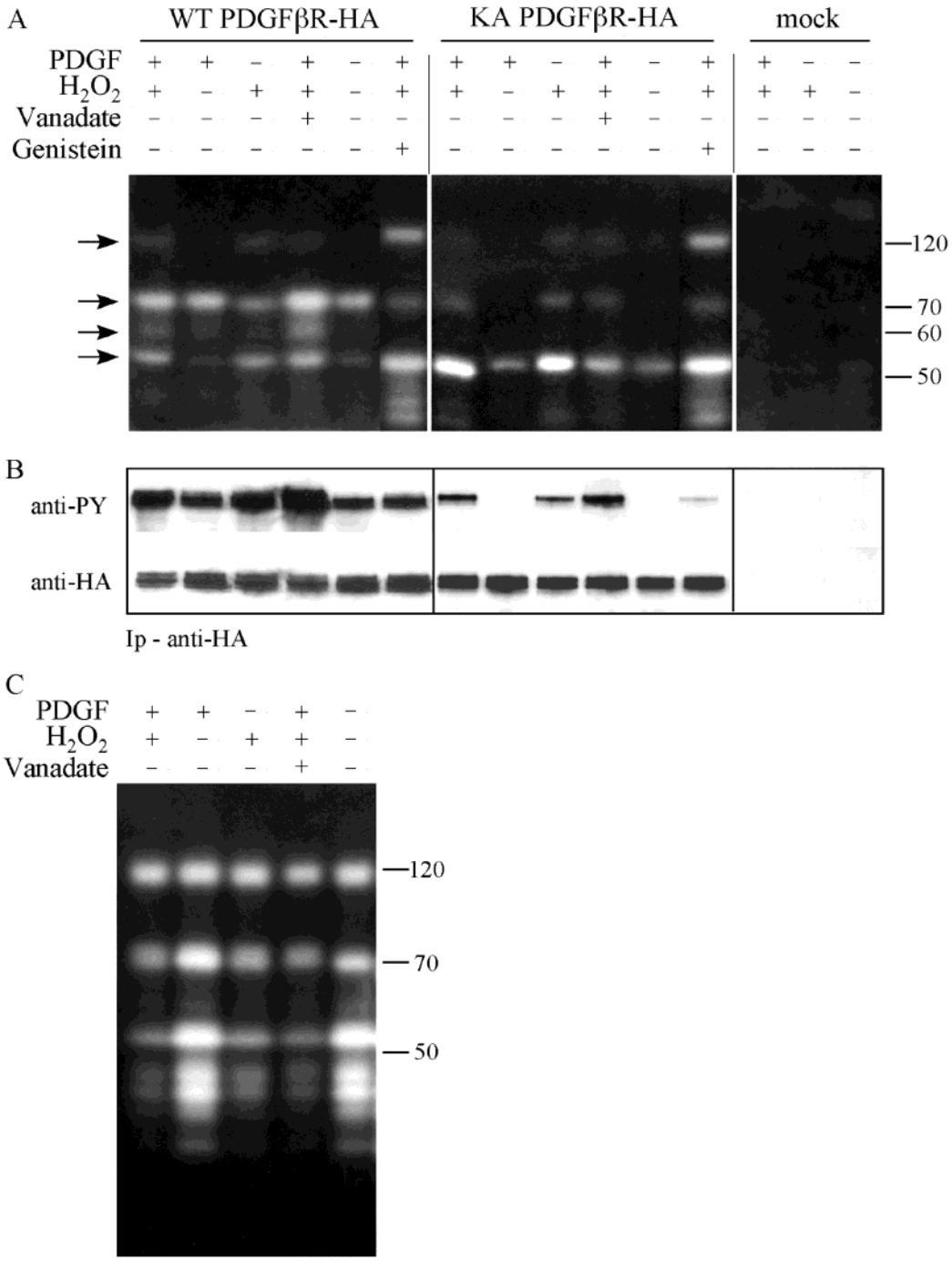

FIGURE 1: PTPs in PDGFβR immunoprecipitates. (A) The HA-tagged PDGFβR wild-type (WT, left panel) and K634A mutant (middle panel) were overexpressed in HEK 293 cells. Cells were pretreated as indicated and extracted, and the PDGFβR was immunoprecipitated with anti-HA antibodies. The immunoprecipitates were separated by SDS−PAGE in a gel containing [^{32}P]tyrosine-phosphorylated poly-(Glu_4Tyr_1), and PTPs were visualized as activity (white) bands after renaturation. Control experiments were performed using mock-transfected cells (right panel) and isotype-matched control IgG (not shown). This picture is assembled from two autoradiograms with matching exposure, obtained under identical conditions. The data are representative of three experiments with consistent results. (B) Aliquots of the immunoprecipitates were used to evaluate tyrosine phosphorylation and the amount of immunoprecipitated receptor. (C) Lysate aliquots were analyzed by in-gel assays for comparison. The assays shown correspond to ~1% of the lysate input into the receptor immunoprecipitations.

sion construct (or mock-transfected) and subjected to various treatments as indicated in Figure 1. These included PDGF stimulation and treatment with H_2O_2. The latter treatment was chosen, since earlier observations had indicated that oxidation-inducing treatment (UV or H_2O_2) stabilized PTP−substrate complexes (*15*, *16*). After lysis of the cells in the absence or presence of sodium orthovanadate (as indicated), the PDGFβR was immunoprecipitated with anti-HA antibodies. To visualize PTPs which coprecipitate together with the PDGFβR, we used the in-gel PTP activity assay described by Burridge and Nelson (*7*). The position of a coprecipitating PTP appears as a white band where ^{32}P had been released by the renatured PTP from the labeled substrate polymerized into the gel.

In the experiment shown in Figure 1A (left panel), four PTP components of ~120, ~70, ~60, and ~53 kDa were

detected in wild-type PDGFβR immunoprecipitates. PDGF stimulation slightly increased the level of association of the 70 kDa PTP with the PDGFβR. H_2O_2 treatment promoted association of 120 and 53 kDa PTPs with the PDGFβR, suggesting an influence of PTP oxidation on the recoverable association. Cell treatment with PDGF and H_2O_2, and addition of sodium orthovanadate to the lysis buffer, strongly increased the PDGFR tyrosine phosphorylation level (Figure 1B), accompanied by an increase in the level of association of the 70 and 60 kDa PTP components. In control experiments with mock-transfected cells (Figure 1A, right panel) or by immunoprecipitation with isotype-matched IgG (not shown), no PTP activity was detectable, confirming specificity of the Ip and the assay. For comparison, we analyzed with an in-gel assay the PTP pattern of the corresponding lysates directly (Figure 1C). The pattern was complex, containing clearly more activity bands than could be detected in the immunoprecipitates. Main components at 120, 70, 60, and 53 kDa were present in proportions different from those in the immunoprecipitates. Both observations suggest that the PTP association with the PDGFβR was selective. PDGF treatment led to a small shift of the 70 kDa PTP component to a position of lower mobility, suggesting its phosphorylation upon PDGF stimulation. Also, this component appears to be somewhat more active in the PDGF-treated cells. It seems therefore possible that part of the increase in the magnitude of the 70 kDa PTP signal in the PDGFβR immunoprecipitates was due to elevated activity after PDGF treatment. H_2O_2 treatment reduced the activity of several components in the lysates, probably by irreversible inactivation. It is known that H_2O_2 treatment can lead to both reversible and irreversible PTP inactivation (*17*). Notably, the activity of the 53 and 120 kDa components was reduced. Thus, increased amounts of these PTPs in the PDGFR immunoprecipitates cannot be explained by elevated activity due to H_2O_2 treatment.

A very similar pattern of PTPs associating with the PDGFβR could be detected in murine fibroblasts (see below).

Dependence of PTP Association on PDGFR Tyrosine Phosphorylation. To further evaluate the role of PDGFR phosphorylation in the association of the various PTP components, we used the kinase-dead PDGFβR K634A mutant for the same type of experiment (Figure 1A, middle panel). When overexpressed in HEK 293 cells, the kinase-dead receptor was not phosphorylated, neither in the absence nor in the presence of ligand. However, stimulation of the cells with H_2O_2 led to K634A PDGFβR phosphorylation, albeit at clearly lower levels than observed with the wild-type receptor. This phosphorylation must occur by the action of other tyrosine kinases since the K634A PDGFβR is completely devoid of kinase activity (*9*). Association of the 70 and 60 kDa components with the K634A PDGFβR was absent under conditions of no receptor phosphorylation, i.e., with no treatment or with PDGF stimulation only. Low levels of K634A PDGFR phosphorylation upon treatment with H_2O_2 led to some detectable association of the 70 kDa PTP component. Taken together, association of the 70 and 60 kDa PTPs with the PDGFR requires PDGFR tyrosine phosphorylation. Interestingly, association of the 120 and 53 kDa components was still apparent with the kinase-dead receptor; the 53 kDa component in fact exhibited an even stronger association. This finding suggests that tyrosine phosphorylation of the PDGFR may not be critical for association of these PTPs. To further evaluate this possibility, association experiments were performed in the presence of genistein, a general tyrosine kinase inhibitor. This compound reduced the level of phosphorylation of the wild-type PDGFR and nearly abrogated the H_2O_2-induced phosphorylation of the kinase-dead PDGFR (Figure 1B). In both cases, the association of the 120 and 53 kDa PTPs with the PDGFR was still apparent and even improved. Thus, PDGFR tyrosine phosphorylation seems not to be required for association of the receptor with these PTPs.

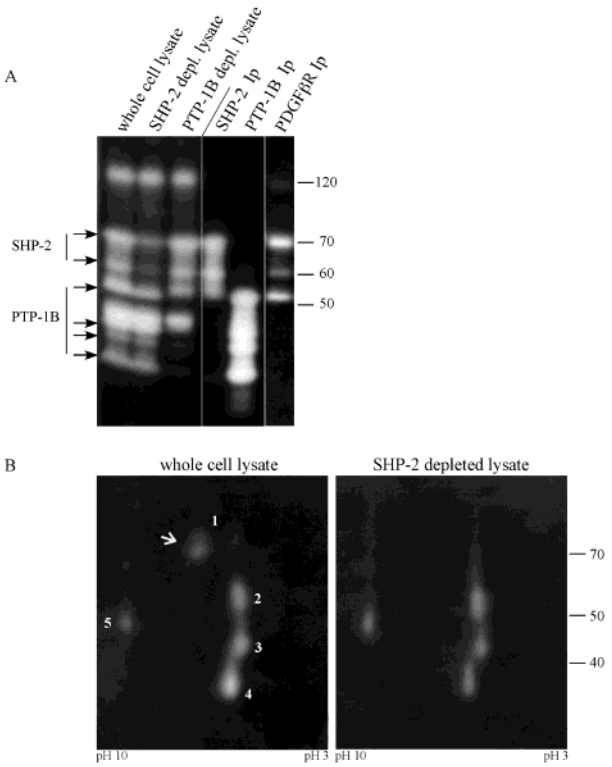

FIGURE 2: Identification of SHP-2 and PTP1B as components in HEK 293 cell lysates by immunodepletion. Cell lysates were incubated with anti-SHP-2 or anti-PTP-1B antibodies (as indicated), and immunocomplexes were precipitated with protein G/A Sepharose. Immunoprecipitates and aliquots of the supernatants (as indicated) were analyzed with a PTP in-gel assay in a one-dimensional gel (A) or two-dimensional gels (B; the example for SHP-2 depletion is shown). PTP-1B and SHP-2 bands (spot) are indicated. The numbers are described in the text. The PDGFβR immunoprecipitate shown for comparison in panel A was obtained from PDGFβR-expressing cells, stimulated with PDGF and H_2O_2.

Identification of PDGFβR-Associating PTPs. To identify the PTPs coprecipitating with the PDGFβR under these different treatment conditions, we first attempted immunoblotting using antibodies against potentially relevant PTPs, including SHP-2, PTP-1B, and TC-PTP. However, only SHP-2, a PTP known to interact with the PDGFR, could be identified (not shown) as representing the 70 kDa band of the in-gel assay (see also below), suggesting that the efficiency of association for the other PTPs is low. We failed to enrich sufficient PTP material by various purification procedures, monitored by in-gel assays, to allow identification of PTPs by mass spectrometry (not shown).

We were, however, successful in identifying PTPs by immunodepletion from cell lysates. Cell lysates were treated with PTP-selective antibodies, and depleted lysates were subsequently analyzed with an in-gel assay. The size of PTP

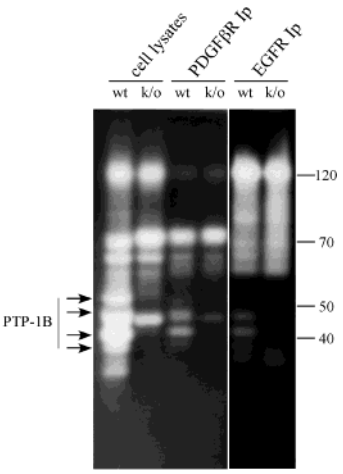

FIGURE 3: PTPs associating with PDGFβR and EGFR in murine fibroblasts. Lysates of immortalized murine PTP-1B knockout fibroblasts, mock-transfected or reconstituted with wild-type human PTP-1B (as indicated), were stimulated with H_2O_2 and PDGF or EGF, respectively, and were subjected to immunoprecipitation with anti-PDGFβR or anti-EGFR antibodies. Lysates and immunoprecipitates were analyzed with a PTP in-gel assay. Different parts of the same gel have been exposed for different lengths of time to optimize PTP detection.

bands (see Figure 1) led us to speculate about their identity and to test specific antibodies for the depletion. According to immunoblotting, an obvious candidate for the 70 kDa PTP band was SHP-2. A potential candidate for the 53 kDa PTP was PTP-1B. The specificity of commercial antibodies for both PTPs was confirmed by MALDI-TOF analysis (see Experimental Procedures). Lysates from HEK 293 cells were incubated with antibodies against SHP-2 or PTP-1B, and aliquots of the supernatants and immunoprecipitates were analyzed with a one-dimensional in-gel assay (Figure 2A). The anti-SHP-2 antibody depleted the 70 and 60 kDa PTPs from the lysate, and corresponding bands appeared in the anti-SHP-2 immunoprecipitate. Since it was important to prove that each activity band represented only a single PTP component, we also analyzed aliquots of cell lysates from depletion experiments on two-dimensional in-gel assays. An example for the SHP-2 depletion is shown in Figure 2B. An activity spot at 70 kDa (spot 1, arrow) disappeared in the anti-SHP-2-depleted lysate. Because of a somewhat reduced sensitivity of the two-dimensional analysis, the 60 kDa component was not detectable in the undepleted lysate. In summary, the 70 kDa band in the PDGFβR immunoprecipitates represents SHP-2 and the 60 kDa band represents most likely an active fragment of SHP-2. This identification is also consistent with the dependence of the association of both components on PDGFR tyrosine phosphorylation (see above).

To our surprise, the monoclonal anti-PTP-1B antibody depleted several (at least four) activity bands from the cell lysate (Figure 2A). Also, a corresponding pattern of four main activity components occurred in the immunoprecipitate. We assumed that the 53 kDa component in this pattern represented the full-length PTP-1B (also seen in the PDGFβR immunoprecipitate) and that the smaller molecules represented active fragments of PTP-1B. To further confirm the identity of these bands, we compared lysates from PTP-1B knockout fibroblasts with those from fibroblasts harboring wild-type PTP-1B (Figure 3). Indeed, the PTP-1B knockout cells also lacked at least four activity bands, further supporting their identity as different forms of PTP-1B. In this cell background, at least three of these bands, now known to represent PTP-1B, were detectable in PDGFβR immunoprecipitates (Figure 3). The fragments are unlikely to have arisen during lysis since direct cell extraction with hot SDS−PAGE sample buffer resulted in the same patterns (not shown). Rather, the extent of PTP-1B fragmentation may depend on the cellular background. It was more pronounced in the PTP-1B retransfected murine knockout cells and HEK 293 cells than in Swiss 3T3 fibroblasts or A431 cells (not shown).

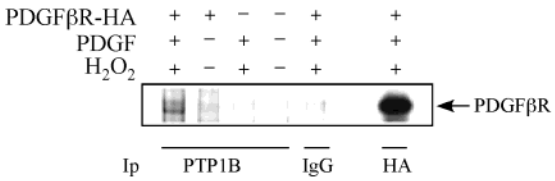

FIGURE 4: Co-immunoprecipitation of the PDGFβR with PTP-1B. HEK 293 cells overexpressing the HA-tagged PDGFβR or control cells were left unstimulated or were stimulated with PDGF and H_2O_2, and cell extracts were subjected to immunoprecipitation with anti-PTP-1B antibodies, isotype-matched control IgG, or anti-HA antibodies as indicated. Immunoprecipitates were subjected to a kinase reaction in the presence of [γ-^{32}P]ATP and analyzed by SDS−PAGE and autoradiography. For a positive control, 5% of a corresponding immunoprecipitate with anti-HA antibodies was loaded.

Detection of association of wild-type PTP-1B with the PDGFβR was surprising. On the basis of detection by immunoblotting and FRET measurements, association of the PDGFβR with PTP-1B can be readily demonstrated if a catalytically inactive PTP-1B "trapping mutant" was used, but not with wild-type PTP-1B (*11*, *18*). We, therefore, wished to confirm association of wild-type PTP-1B with the PDGFβR by an independent method. PTP-1B was immunoprecipitated, and to detect the associated PDGFβR, the immunoprecipitate was subjected to a kinase reaction. A 180 kDa phosphoprotein, comigrating with the phosphorylated PDGFβR, is coprecipitated with PTP-1B from HEK 293 cells overexpressing the PDGFβR, provided the cells are pretreated with H_2O_2, but not from mock-transfected cells (Figure 4). Consistent with the in-gel assay data, this experiment suggests formation of a wild-type PTP-1B−PDGFβR complex.

In the course of the depletion experiments, presented in Figure 2, we observed that one of the PTP bands in the 45 kDa region was not or only partially depleted by anti-PTP-1B antibody treatment. Also, there was a band of this size detectable in PTP-1B knockout fibroblasts (Figure 3). We noticed that this PTP had a completely different isoelectric point in two-dimensional PAGE: spot 5 with a pI of ~8 compared to a pI of ~5.8 for spots 2−4 representing PTP-1B (Figure 2B). These observations indicated that there is another PTP, whose mobility somewhat overlaps with the mobility of one of the PTP-1B fragments. A size candidate PTP for this activity was TC-PTP. TC-PTP occurs in different isoforms which, according to databases and literature (*19*), have a pI of 8.6−8.9 and a size of 45−48 kDa. To identify the 45 kDa band as TC-PTP, we first removed PTP-1B by immunodepletion and subjected the PTP-1B-depleted lysate to a second cycle of depletion, this time for TC-PTP. Indeed, the 45 kDa band persisting in the PTP-1B-depleted lysate was removed by treatment with the anti-

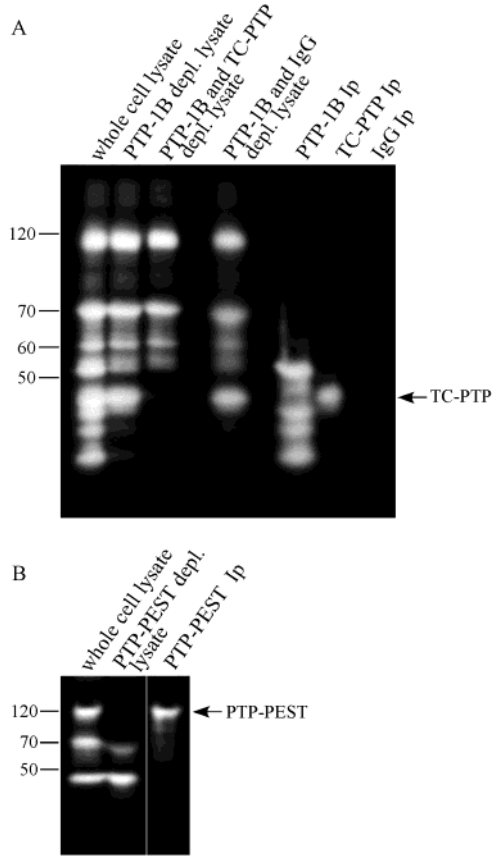

FIGURE 5: Identification of TC-PTP and PTP-PEST by immunodepletion. (A) Aliquots of the HEK 293 cell lysate were left untreated, were incubated with anti-PTP1B antibody only, or were incubated with the anti-TC-PTP antibody or the isotype-matched IgG control antibody after PTP-1B depletion (as indicated). Corresponding immunoprecipitates were applied in the last three lanes. The position of TC-PTP is marked. (B) Aliquots of the cell lysate from immortalized murine PTP-1B knockout fibroblasts were left untreated or incubated with the anti-PTP-PEST antibody (as indicated). The corresponding immunoprecipitate is shown in the last lane. The position of PTP-PEST is marked.

TC-PTP antibody. Immunoprecipitated TC-PTP appeared as a single activity band at 45 kDa (Figure 5A). Inspection of PDGFβR immunoprecipitates from PTP-1B knockout cells revealed that the 45 kDa component, now identified as TC-PTP, is also detectable, albeit weakly (Figure 3).

Finally, the same strategy of immunodepletion was used to identify the 120 kDa PTP activity coprecipitating with the PDGFβR (Figure 1). As known from experiments with recombinant PTPs, the renaturation of transmembrane PTPs, required for detection in the in-gel activity assay, is not effective and their detection succeeds only with low sensitivity (*7*). Therefore, we disregarded membrane PTPs and searched for cytoplasmic PTPs of the appropriate size. Although the ubiquitously expressed PTP-PEST has a molecular mass of 88 kDa, it is known that its high proline content (11% of the amino acids) yields an apparent mobility on SDS−PAGE of ~115−120 kDa (*20*). For the corresponding depletion experiments (Figure 5B), we used immortalized murine PTP-1B knockout fibroblasts to reduce the complexity of the cell lysate. Incubation with anti-PTP-PEST antibodies indeed completely depleted the 120 kDa PTP from the cell lysate, thus proving it was PTP-PEST.

Taken together, SHP-2, PTP-1B, TC-PTP, and PTP-PEST were identified as PTPs immunoprecipitating with the PDGFβR.

PTPs Associating with Other RTKs. To evaluate the possible relevance of the PTPs found in association with the PDGFβR, we compared the PDGβR with other RTKs in the same type of assay. Interestingly, immunoprecipitation of the EGFR from the same type of fibroblasts clearly yielded patterns of PTP association different from that obtained with the PDGFβR (Figure 3). In EGFR immunoprecipitates, mainly PTP-PEST was found, weakly PTP-1B, very weakly TC-PTP, and no SHP-2. In contrast, the predominant PTPs associating with the PDGFβR were SHP-2 and PTP-1B.

We also investigated PTPs associated with c-Kit, an RTK structurally related to the PDGFβR. Since HEK 293 cells represent a nonphysiological cell background for c-Kit, we instead analyzed PTP association with this RTK in CHRF cells, a myeloid leukemia line, which expresses high endogenous levels of c-Kit. As a negative control line, we used K562 cells, which have a similar PTP expression pattern (Figure 6A) but express very low levels of c-Kit (Figure 6B). Cells were pretreated as indicated, and c-Kit was immunoprecipitated. As shown in Figure 6A, PTP association with c-Kit was strongly dependent on ligand stimulation, and the main components in the immunoprecipitates had sizes of ~120, ~72−75, and 68 kDa. Very weak bands of 53 and 45 kDa were also detectable. By inference from our identification experiments in fibroblast lysates, the 120 kDa PTP is likely to represent PTP-PEST, and the weak bands of 53 and 45 kDa are likely to represent PTP-1B and TC-PTP, respectively. The band running above the 70 kDa position is most likely a heavily phosphorylated species of SHP-2, which shifts to a lower mobility upon phosphorylation. In addition to this set of PTPs, there was one more phosphatase of ~68 kDa, which we suspected to represent SHP-1. In lanes where c-Kit immunoprecipitates from K562 cells, i.e., mock precipitates had been applied, no PTP activity was detectable, demonstrating the specificity of the in-gel assay for c-Kit-associating PTPs. To identify the 68 kDa PTP, we subjected CHRF cell lysates to immunodepletion with SHP-1 antibodies (Figure 6C). Immunoprecipitation of SHP-1 with the antibody that was used was very selective but rather inefficient. While a weak 68 kDa activity band appears in the SHP-1 immunoprecipitates, only incomplete reduction of the 68 kDa band in lysates was achieved, while the 72 kDa band was not affected. We, therefore, conclude that the 68 kDa activity band in c-Kit immunoprecipitates was most likely identical with SHP-1.

DISCUSSION

Biological Relevance of PTP Association with the PDGFβR. By co-immunoprecipitation combined with immunodepletion, individual immunoprecipitation, and the use of knockout cells, we identified five PTPs, which interact with the PDGFβR. The major entities detected are SHP-2 and PTP-1B. SHP-2 has been established earlier as a PDGFβR-interacting molecule. Still, its physiological role is not properly understood. Roles both in mediating PDGFβR signals and in negatively regulating receptor signaling have been proposed (*2*). Recently, Meng et al. (*21*) reported transient inactivation of SHP-2 after PDGF stimulation, using

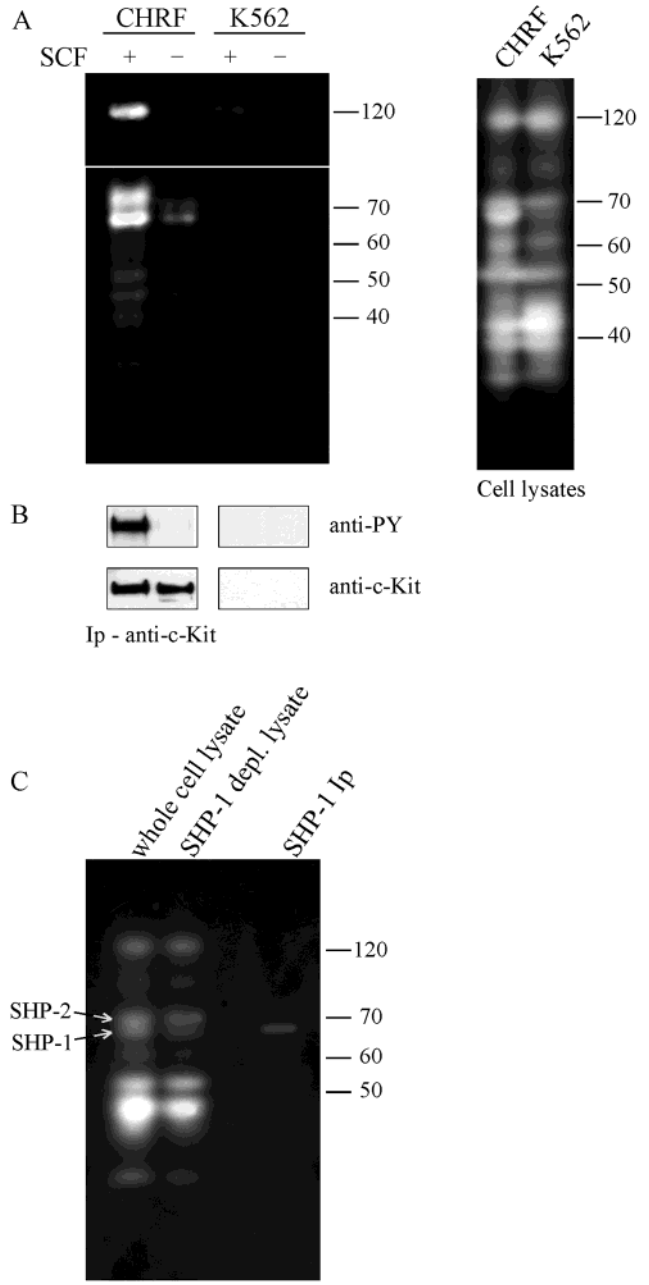

FIGURE 6: Association of PTPs with c-Kit. (A) CHRF and K562 cells were pretreated with H_2O_2 and then stimulated with SCF or left untreated (as indicated). The c-Kit receptor was immunoprecipitated, and immunoprecipitates were analyzed with an in-gel assay. Different parts of the same gel have been exposed for different lengths of time to optimize PTP detection. For comparison, lysate aliquots of CHRF and K562 cells were directly analyzed with a PTP in-gel assay (right panel). (B) Aliquots of the immunoprecipitates were used to evaluate tyrosine phosphorylation and the amount of immunoprecipitated receptor. (C) Aliquots of the CHRF cell lysate were left untreated or were immunodepleted with anti-SHP-1 antibodies (as indicated). The corresponding SHP-1 immunoprecipitate was applied in the last lane. Positions of SHP-2 and SHP-1 are marked.

a modified PTP in-gel assay protocol. From these data, a negative role of SHP-2 for PDGFR signaling and inactivation of SHP-2 as an aspect of signal generation have been inferred.

According to earlier data, PTP-1B clearly has the capacity to downregulate PDGFR signaling (*22*, *23*). Interestingly, in PTP-1B knockout cells, PDGF receptors are hyperphosphorylated, strongly suggesting a negative role of PTP-1B in the regulation of signaling (*18*). The receptor association of PTP-1B described here is consistent with these observations and with a physiological role of PTP-1B in the regulation of signaling. However, no cellular or organismic phenotype by PTP-1B knockout has yet been attributed to PDGFR hyperphosphorylation (*18*). This finding may be related to another observation of our study, the association of the PDGFβR with further PTPs such as PTP-PEST and TC-PTP. Thus, elimination of a single PTP may be insufficient in leading to a biological phenotype in respective knockout cells. In fact, the in-gel analysis of RTK−PTP association described here uncovers multiple RTK−PTP interactions. Since the in-gel assay misses detection of other potentially specific PDGFR interaction partners, the number of involved PTPs may be even greater. For example, our assays did not reveal DEP-1 or LMW-PTP, phosphatases which have been shown earlier to negatively regulate the PDGFR in transfection studies (*8*, *24*).

For TC-PTP, an interaction with the PDGFR has previously not been reported. Suggested by our association data, evaluation of its possible participation in the regulation of PDGFβR signaling seems highly warranted.

Mechanism of PTP-1B−PDGFβR Association. Complexes of active wild-type PTPs and their substrates are unstable since they are rapidly decomposed by the enzyme's action (*25*). Consistent with earlier data (*11*), no association of wild-type PTP-1B with the PDGFβR could be detected by immunoblotting while the in-gel phosphatase assay uncovered specific association. Consistent with coprecipitation of PTP-1B activity with the PDGFβR, we could also detect the PDGFβR in PTP-1B immunoprecipitates using an autokinase assay for detection. Pretreatments of cells with H_2O_2 strongly improved the co-immunoprecipitation recovery of PTP-1B with the PDGFβR. We have previously obtained evidence that oxidation stabilized PTP−RTK association (*15*, *16*). As one possible explanation, we have proposed that a PTP with an oxidized catalytic cysteine could form a more stable complex with the RTK, similar to "substrate trapping" mutations in the catalytic domain (*16*). We have to consider a second possibility. Interestingly, association of PTP-1B and PTP-PEST also occurred with the kinase-dead PDGFβR K634A mutant and was even enhanced in the presence of the general tyrosine kinase inhibitor genistein. These findings suggest that the association we observed here does not primarily occur via an interaction of the PTP catalytic domain with receptor phosphotyrosines. Still, PTP modification by oxidation seems to be necessary for binding. This situation is somewhat reminiscent of PTP-1B binding to the insulin receptor or integrins (*26*, *27*) and PTP-PEST binding to its substrate $p130^{CAS}$ (*28*). In these studies, formation of a complex with the respective interaction partners was only demonstrable or greatly enhanced when catalytically inactive PTP variants were employed; however, PTP domains which do not recognize phosphotyrosine take part in the association. In the case of PTP-1B, two domains which are important for target binding were identified, a YY-containing sequence in the N-terminus which is important for binding to the insulin receptor and a proline-rich domain in the C-terminus which is a SH3 domain ligand and required for downregulation of integrin signaling (*26*, *27*). One can speculate that one of these domains may participate in direct or indirect

binding of PTP-1B to the PDGFβR. TC-PTP lacks a proline-rich domain, and this may, in part, explain the much weaker association with the PDGFβR compared to that of PTP-1B. Another phosphotyrosine-independent association of PTP-1B has recently been described, association with E-cadherin (*29*). These authors identified a 20-amino acid sequence in the E-cadherin cytoplasmic domain, which is required for PTP-1B binding. The motif in PTP-1B which is required for interaction has not yet been identified. Interestingly, two sequences in the PDGFβR, amino acids 728−742 and 1045−1061, are similar to the respective E-cadherin sequence, and their possible participation in PTP-1B association needs to be investigated.

How H_2O_2 may stabilize phosphotyrosine-independent PTP−RTK complexes is an open question. Potentially, H_2O_2 treatment could cross-link PTP-1B to the RTKs through formation of disulfide bridges (*16*). Indeed, PTP activity with a high molecular weight could be seen in PDGFR immunoprecipitates from H_2O_2-treated cells co-overexpressing the PDGFβR and wild-type PTP-1B when run under nonreducing but not under reducing conditions and not in the absence of H_2O_2 treatment (B. Markova, unpublished data). Alternatively, H_2O_2 treatment may improve RTK−PTP association by oxidative modification of the interaction domains described above. Whatever the mechanism of stabilization, the results suggest that a fraction of PTP molecules is sufficiently close to the PDGFβR to allow complex formation and co-immunoprecipitation.

Possible Relevance of PTP Fragments. Interestingly, the in-gel assay detected active fragments of PTP-1B and SHP-2. The fragmentation complicates the pattern of activity bands. The PTP fragments are apparently no artifacts of the solubilization procedure and already exist in the cells. We believe that it is the high sensitivity of the in-gel assay and likely increased activity or improved activity recovery of the PTP fragments which made their detection possible. For example, we detected further fragments of PTP-1B, in addition to the previously known 37 and 42 kDa degradation products (*30*, *31*). In fibroblasts, we observed that the active PTP-1B fragments associated apparently better than full-length PTP-1B with the PDGFβR. One possible explanation for this may be their better access to the receptor. Full-length PTP-1B is anchored in the endoplasmic reticulum. The 42 kDa PTP-1B fragment is the result of C-terminal cleavage by calpain and is released from its anchoring in the endoplasmic reticulum (*31*). Similarly, other PTP-1B fragments may also not be bound to cellular structures and thus be more readily available for PDGFβR interaction. These findings suggest to us to further examine the nature and functional relevance of the PTP cleavage reactions. Accessibility may also affect the recovery of TC-PTP in the RTK immunoprecipitates. This PTP is mainly localized in the nucleus which may compromise RTK interaction under our conditions of cell treatment (*32*).

Selectivity and Redundancy of RTK−PTP Interaction. Comparing different RTKs for association with PTPs, we observed some overlapping specificities. If one considers, however, quantities of detectable PTP activity, the different RTKs exhibit characteristic individual patterns of PTP association (Table 1). As seen with c-Kit, the pattern of PTPs is affected by the cellular background and may also be somewhat affected by the antibodies used for immunoprecipitation. Still, the differences seen are impressive and are in line with previous data implicating roles for some of the identified PTPs in RTK signaling (Table 1). Also, the interaction mechanisms seem to differ for some of the RTK−PTP associations. For example, PTP-PEST binds to the PDGFβR with relatively low efficiency and only in the presence of H_2O_2. Its association with the EGFR is strong and not dependent on ligand stimulation or H_2O_2 treatment. PTP-PEST is known to bind effectively via a proline-rich domain to an SH3 domain of Grb2 and through Grb2 indirectly to the EGFR. Interestingly, very similar to our findings with the in-gel assays, Charest et al. also report that the association is independent of EGFR ligand stimulation (*33*). PTP-PEST association with c-Kit is moderate, depends on H_2O_2, and is strongly enhanced by ligand stimulation. SHP-1 and SHP-2 are established interaction partners of c-Kit (*34*, *35*). An association of PTP-PEST with c-Kit has to our knowledge previously not been reported. Our findings strongly suggest that the role of PTP-PEST for c-Kit signaling should be analyzed.

Table 1: Differential Association of PTPs with Different RTKs As Revealed by PTP in-Gel Assays[a]

	PDGFβR	EGFR	c-Kit
PTP-PEST	+	+++	++
effect on signaling	not known	not known	**not known**
SHP-2	+++	−	++
effect on signaling	positive (*36*, *37*) or negative (*21*, *38*)		positive (*39*)
SHP-1	na[b]	na[b]	+++
effect on signaling			negative (*34*)
PTP-1B	++	+	±
effect on signaling	negative (*18*)	negative (*18*)	
TC-PTP	++	±	−
effect on signaling	**not known**	negative (*32*)	

[a] Previously not described interactions are highlighted in bold. [b] The PDGFβR and the EGFR were compared in fibroblasts. Therefore, information about SHP-1, which is not expressed in fibroblasts, cannot be obtained in these assays (na, not analyzed).

ACKNOWLEDGMENT

We greatly acknowledge the provision of various reagents by Drs. F. Haj, B. Neel, N. Tonks, M. Tremblay, and M. Lieberman. We are very grateful to Dr. Ulf Hellman for training and technical support in mass spectrometry and to Christiane Burkhardt for help with PTP-PEST identification.

REFERENCES

1. Schlessinger, J. (2000) *Cell 103*, 211−225.
2. Östman, A., and Böhmer, F. D. (2001) *Trends Cell Biol. 11*, 258−266.
3. Elchebly, M., Payette, P., Michaliszyn, E., Cromlish, W., Collins, S., Loy, A. L., Normandin, D., Cheng, A., Himms-Hagen, J., Chan, C. C., Ramachandran, C., Gresser, M. J., Tremblay, M. L., and Kennedy, B. P. (1999) *Science 283*, 1544−1548.
4. Klaman, L. D., Boss, O., Peroni, O. D., Kim, J. K., Martino, J. L., Zabolotny, J. M., Moghal, N., Lubkin, M., Kim, Y. B., Sharpe, A. H., Stricker-Krongrad, A., Shulman, G. I., Neel, B. G., and Kahn, B. B. (2000) *Mol. Cell. Biol. 20*, 5479−5489.
5. Chiarugi, P., Cirri, P., Taddei, M. L., Talini, D., Doria, L., Fiaschi, T., Buricchi, F., Giannoni, E., Camici, G., Raugei, G., and Ramponi, G. (2002) *J. Cell Sci. 115*, 2219−2232.
6. Andersen, J. N., Mortensen, O. H., Peters, G. H., Drake, P. G., Iversen, L. F., Olsen, O. H., Jansen, P. G., Andersen, H. S., Tonks, N. K., and Møller, N. P. (2001) *Mol. Cell. Biol. 21*, 7117−7136.
7. Burridge, K., and Nelson, A. (1995) *Anal. Biochem. 232*, 56−64.

8. Kovalenko, M., Denner, K., Sandstrom, J., Persson, C., Gross, S., Jandt, E., Vilella, R., Böhmer, F., and Östman, A. (2000) *J. Biol. Chem. 275*, 16219−16226.
9. Sorkin, A., Westermark, B., Heldin, C. H., and Claesson-Welsh, L. (1991) *J. Cell Biol. 112*, 469−478.
10. Tenev, T., Böhmer, S. A., Kaufmann, R., Frese, S., Bittorf, T., Beckers, T., and Böhmer, F. D. (2000) *Eur. J. Cell Biol. 79*, 261−271.
11. Haj, F. G., Verveer, P. J., Squire, A., Neel, B. G., and Bastiaens, P. I. (2002) *Science 295*, 1708−1711.
12. Chen, C., and Okayama, H. (1987) *Mol. Cell. Biol. 7*, 2745−2752.
13. Harlow, E., and Lane, D. (1999) *Using antibodies: a laboratory manual*, Cold Spring Harbor Laboratory Press, Plainview, NY.
14. Hellman, U. (2000) *EXS 88*, 43−54.
15. Gross, S., Knebel, A., Tenev, T., Neininger, A., Gaestel, M., Herrlich, P., and Böhmer, F. D. (1999) *J. Biol. Chem. 274*, 26378−26386.
16. Herrlich, P., and Böhmer, F. D. (2000) *Biochem. Pharmacol. 59*, 35−41.
17. Denu, J. M., and Tanner, K. G. (1998) *Biochemistry 37*, 5633−5642.
18. Haj, F. G., Markova, B., Klaman, L. D., Böhmer, F. D., and Neel, B. G. (2003) *J. Biol. Chem. 278*, 739−744.
19. Ibarra-Sanchez, M. J., Simoncic, P. D., Nestel, F. R., Duplay, P., Lapp, W. S., and Tremblay, M. L. (2000) *Semin. Immunol. 12*, 379−386.
20. Charest, A., Wagner, J., Shen, S. H., and Tremblay, M. L. (1995) *Biochem. J. 308*, 425−432.
21. Meng, T. C., Fukada, T., and Tonks, N. K. (2002) *Mol. Cell 9*, 387−399.
22. Lammers, R., Bossenmaier, B., Cool, D. E., Tonks, N. K., Schlessinger, J., Fischer, E. H., and Ullrich, A. (1993) *J. Biol. Chem. 268*, 22456−22462.
23. Liu, F., and Chernoff, J. (1997) *Biochem. J. 327*, 139−145.
24. Chiarugi, P., Cirri, P., Raugei, G., Camici, G., Dolfi, F., Berti, A., and Ramponi, G. (1995) *FEBS Lett. 372*, 49−53.
25. Flint, A. J., Tiganis, T., Barford, D., and Tonks, N. K. (1997) *Proc. Natl. Acad. Sci. U.S.A. 94*, 1680−1685.
26. Dadke, S., Kusari, J., and Chernoff, J. (2000) *J. Biol. Chem. 275*, 23642−23647.
27. Dadke, S., and Chernoff, J. (2002) *Biochem. J. 364*, 377−383.
28. Garton, A. J., Burnham, M. R., Botuon, A. H., and Tonks, N. K. (1997) *Oncogene 15*, 877−885.
29. Xu, G., Arregui, C., Lilien, J., and Balsamo, J. (2002) *J. Biol. Chem. 107*, 1.
30. Charbonneau, H., Tonks, N. K., Kumar, S., Diltz, C. D., Harrylock, M., Cool, D. E., Krebs, E. G., Fischer, E. H., and Walsh, K. A. (1989) *Proc. Natl. Acad. Sci. U.S.A. 86*, 5252−5256.
31. Frangioni, J. V., Oda, A., Smith, M., Salzman, E. W., and Neel, B. G. (1993) *EMBO J. 12*, 4843−4856.
32. Tiganis, T., Kemp, B. E., and Tonks, N. K. (1999) *J. Biol. Chem. 274*, 27768−27775.
33. Charest, A., Wagner, J., Kwan, M., and Tremblay, M. L. (1997) *Oncogene 14*, 1643−1651.
34. Kozlowski, M., Larose, L., Lee, F., Le, D. M., Rottapel, R., and Siminovitch, K. A. (1998) *Mol. Cell. Biol. 18*, 2089−2099.
35. Tauchi, T., Feng, G. S., Marshall, M. S., Shen, R., Mantel, C., Pawson, T., and Broxmeyer, H. E. (1994) *J. Biol. Chem. 269*, 25206−25211.
36. Bennett, A. M., Tang, T. L., Sugimoto, S., Walsh, C. T., and Neel, B. G. (1994) *Proc. Natl. Acad. Sci. U.S.A. 91*, 7335−7339.
37. Rönnstrand, L., Arvidsson, A. K., Kallin, A., Rorsman, C., Hellman, U., Engstrom, U., Wernstedt, C., and Heldin, C. H. (1999) *Oncogene 18*, 3696−3702.
38. Saxton, T. M., Henkemeyer, M., Gasca, S., Shen, R., Rossi, D. J., Shalaby, F., Feng, G. S., and Pawson, T. (1997) *EMBO J. 16*, 2352−2364.
39. Qu, C. K., Shi, Z. Q., Shen, R., Tsai, F. Y., Orkin, S. H., and Feng, G. S. (1997) *Mol. Cell. Biol. 17*, 5499−5507.

BI0265574